PAPER

Study of the ^{33}Cl spectroscopic factors via the ^{32}S(^{3}He, d)^{33}Cl one-proton transfer reaction

IOP Publishing Journal of Physics G: Nuclear and Particle Physics
J. Phys. G: Nucl. Part. Phys. **48** (2021) 065101 (16pp) https://doi.org/10.1088/1361-6471/abdee4

Study of the ^{33}Cl spectroscopic factors via the ^{32}S(^{3}He, d)^{33}Cl one-proton transfer reaction

I Lombardo[1,*], D Dell'Aquila[2,3], M Cinausero[4], L R Gasques[5], M Vigilante[6,7], V A B Zagatto[8], S Barlini[9,10], R Bolzonella[11], M Bruno[12,13], A Buccola[9,10], A Camaiani[9,10], S M Carturan[4,11], G Casini[9], C Ciampi[9,10], M Cicerchia[4], M D'Andrea[1], M Degerlier[14], D Fabris[15], C Frosin[9,10], F Gramegna[4], A Lepine-Szily[5], G Maggioni[4,11], G Mantovani[4,11,16], T Marchi[4], A Ordine[7], P Ottanelli[9,10], G Pasquali[9,10], S Piantelli[9], V Rigato[4], M Russo[1,17], L Scomparin[11], S Valdrè[9] and G Verde[1]

[1] INFN-Sezione di Catania, Catania, Italy
[2] Dipartimento di Chimica e Farmacia, Università degli Studi di Sassari, Sassari, Italy
[3] INFN-Laboratori Nazionali del Sud, Catania, Italy
[4] INFN-Laboratori Nazionali di Legnaro, Legnaro, Italy
[5] Instituto de Fisica da Universidade de Sao Paulo, 05508-090 Sao Paulo, Brazil
[6] Università degli Studi di Napoli 'Federico II', Napoli, Italy
[7] INFN-Sezione di Napoli, Napoli, Italy
[8] Instituto de Fisica—Universidade Federal Fluminense—Niterói, Brazil
[9] INFN-Sezione di Firenze, Firenze, Italy
[10] Università degli Studi di Firenze, Firenze, Italy
[11] Università degli Studi di Padova, Padova, Italy
[12] Università degli Studi di Bologna, Bologna, Italy
[13] INFN-Sezione di Bologna, Bologna, Italy
[14] Science and Art Faculty, Physics Department, Nevsehir Haci Bektas Veli Univ., Nevsehir, Turkey
[15] INFN-Sezione di Padova, Padova, Italy
[16] Universidade de Santiago de Compostela, Santiago de Compostela, Spain
[17] Università degli Studi di Catania, Catania, Italy

E-mail: ivano.lombardo@ct.infn.it

Received 19 December 2020, revised 21 January 2021
Accepted for publication 22 January 2021
Published 20 April 2021

Abstract

In this paper we discuss new experimental data on the one-proton transfer reaction ^{32}S(^{3}He, d)^{33}Cl* at 9.68 MeV bombarding energy. An enriched ^{32}S

*Author to whom any correspondence should be addressed.

target and a high-granularity hodoscope were used to obtain data for proton transfer reactions to bound and unbound states in ^{33}Cl. Angular distributions were interpreted by means of finite-range DWBA and coupled-channel calculations. The obtained spectroscopic factors have been compared with previous results reported in the literature and with shell model calculations.

Keywords: proton transfer reactions, spectroscopic factors, DWBA and CRC calculations

(Some figures may appear in colour only in the online journal)

1. Introduction

In the last three decades, the structure of light-to-medium mass nuclei has been the subject of a renewed interest, especially thanks to the recent development of radioactive beam facilities, (see, e.g. [Cas00]). The occurrence of exotic phenomena in their structure (see, e.g. [Ots20]), the appearance of molecular effects in light nuclei (see, e.g. [Bij20, Fre18, Lom18]) and their impact on nuclear astrophysics (see, e.g. [Des07, Lom14, HeJ18, Lom19]), stimulated the design of a new generation of particle detectors, particularly well-suited to produce high-resolution data of nuclear reactions (see, e.g. [Aco16, Del19, Pas17, Val19]).

Among the various existing experimental tools, one-nucleon transfer reactions are one of the most powerful ways that can be used to unveil the structure of light-to-medium mass nuclei (see, e.g. [Han03, Hod71]). In particular, it is possible to benchmark the predictions of several shell models obtained using different types of interactions [Tsa05]. In this framework, the determination of the orbital angular momentum of the single particle levels and the extraction of spectroscopic factors C^2S can be obtained by comparing experimental data with distorted-wave Born approximation (DWBA) or coupled reaction channels (CRC) calculations, two well-known theoretical tools that are commonly used in nuclear physics [Aus70, Tho09].

There is another interesting application linked to the estimate of spectroscopic factors. They can be determined experimentally in a direct way also for particle-unbound states that are very close to the separation energy threshold. Furthermore, the C^2S is linked to the partial width Γ_i of the unbound state by the simple formula $\Gamma_i = C^2S \cdot \frac{2\hbar^2}{\mu R^2}\mathbb{P}_\ell\theta_i^2$ [Ili01]. Here, μ is the reduced mass of the particle + core system, R is its channel radius, $\mathbb{P}_\ell$ the penetrability (corresponding to a given orbital angular momentum) and θ_i^2 is the dimensionless single-particle reduced width, that can be easily calculated by solving the Schrodinger equation for a potential well representing the particle + core system [Ili01]. Since all the above mentioned quantities can be calculated, if one knows experimentally the C^2S value for a given state, it is possible to estimate the corresponding partial width Γ_i. This opportunity is particularly interesting for unbound states that are very close to the particle separation threshold; in this case, in fact, the estimate of Γ_i by means of low energy compound nucleus reactions is made difficult by the huge *hindrance* of cross section given by the Coulomb barrier, and direct experiments are often impossible.

Among the various possible physical cases available with stable beams, we fixed our attention to the ^{32}S(^{3}He, d)^{33}Cl reaction; at bombarding energies slightly above the Coulomb barrier it is possible to populate states in the proton-rich ^{33}Cl residual nucleus from the ground state (GS) up to unbound states at ≈ 3 MeV [End77]. Since the 16 protons of ^{32}S fill all the shells up to the $2s_{1/2}$, the extra proton transferred with the (^{3}He, d) reaction can probe the single-particle structure of ^{33}Cl states with respect to the population of the $1d_{3/2}$, $1f_{7/2}$ and $2p_{3/2}$ shells [Ing75, Mor70]. In the $A \approx 30$, $Z \approx 16$ region of the Segrè chart (the zone of the so

called *sd*-nuclei), the universal SD-shell interaction (USD, proposed by Wildenthal in the '80 [Wil82]) had good success in reproducing the binding energies of such nuclides and some of the spectroscopic factors for the low-lying excited states (see, e.g. [Ver94]). However, some other different approaches have been reported in the literature for *sd*-nuclei. As an example, the intermediate-coupling vibrational model (ICVM) by Castel *et al* considers the coupling between quasi-particles and anharmonic core vibrations [Cas71]. As pointed out in references [Ing75, Mor70], the USD and ICVM approaches predict quite different C^2S values for the first low-lying states in the proton rich-nucleus ^{33}Cl, and a comparison with experimental values is necessary to discriminate between the models. Unfortunately, the experimental works aiming at deriving the C^2S values from transfer data show quite strong differences, that go from $\approx 10\%$ up to a factor ≈ 2, as it can be seen in references [Gra66, Ing75, Koz72, Mor70, Ver94].

From the point of view of nuclear astrophysics, proton-unbound states in ^{33}Cl are populated in the ^{32}S(p,γ)^{33}Cl capture reaction, that is involved in the *rp*-process [Ili92]. In particular, it is shown in reference [Ili92] that the reaction rate at temperatures lower than 0.1 GK is fully dominated by the resonant contribution due to the 2.352 MeV excited state. Since this state is unbound by just 75 keV, it is nearly impossible to measure its contribution to the ^{32}S(p,γ)^{33}Cl reaction via direct experiments. However, the reaction rate due to this resonance can be estimated by knowing its *strength* $\omega\gamma$, that is related to the partial widths Γ_p and Γ_γ. The Coulomb barrier strongly suppresses the Γ_p value, and therefore the Γ_γ radiative width is practically identical to the total width Γ. On the other side, the Γ_p value can be inferred by using the C^2S_p spectroscopic factor, the penetrability and dimensionless proton reduced width, as discussed at the beginning of the paragraph.

For this case, C^2S_p values of 0.061 and 0.07 were reported in two different one-proton transfer experiments [Elb72, Koz72]. Since the transition is weak, the data analysis can be difficult because of the presence of a large background given by close-lying peaks and/or by the presence of contaminants in the target; as an example, the natural sulphur itself is contaminated by ^{34}S ($\approx 4.2\%$) and, to a lower extent, by ^{33}S ($\approx 0.75\%$). New, higher sensitivity, data on this transition would be therefore useful to better constrain the reaction rate of radiative proton capture by sulphur at low temperatures.

In this paper, we describe a new high-resolution measurement of the one-proton transfer on ^{32}S by means of the ^{32}S(^{3}He, d)^{33}Cl reaction at a bombarding energy around 10 MeV. This relatively low energy value allows us to neglect the effect of ^{3}He direct break-up ($Q_{\mathrm{break-up}} \simeq -5.5$ MeV), which would add a continuum contribution to the deuteron spectrum. The experiment is performed exploiting a high-purity target and a new generation hodoscope of silicon detectors, enabling to minimize the effect of undesired contaminant reactions.

The paper is organized as follows. In section 2 we discuss the details of the experimental apparatus here used and of the manufacturing and testing phases of the targets. In sections 3 and 4 we discuss the data reduction phase and the analysis of angular distributions by means of the DWBA and CRC nuclear reaction tools. Finally, we discuss the obtained spectroscopic factors and compare them with previous estimates reported in the literature.

2. Experimental setup

The experiment was performed at the CN van de Graaf accelerator of INFN—Laboratori Nazionali di Legnaro, Italy. A ^{3}He^{++} beam was extracted from an RF source and then accelerated up to 9.68 MeV. The beam energy resolution was of the order of 2 keV, and no traces of contaminants were present after the analysing magnet. The beam was sent to a vacuum chamber of about 35 cm radius, with a vacuum level of the order of 10^{-6} mbar. At the target point, the beam spot diameter was of ≈ 2 mm.

2.1. Target manufacturing and characterization

Targets used for this experiment were made by a natural carbon foil with evaporation of ZnS powder, enriched at 99.9% level in ^{32}S to avoid contaminant peaks due to unwanted reactions on ^{33,34}S. Zn nanocrystals were synthesized using the approach described in reference [Pol08]. Zn nanopowder (size of nanoparticles: 40–80 nm) was weighed and mixed with isotopically enriched sulphur powder in stoichiometric ratio. The procedure was done in a glove box under nitrogen flowing and low humidity, to avoid the ignition of Zn nanopowder. The mixture was poured into a steel tube reactor with caps; then the tube was closed tightly and inserted in the tube furnace. The treatment was performed under nitrogen flow (30 sccm), according to the following scheme: (1) heating at a rate 10 °C min^{-1}, up to 650 °C; (2) dwell at 650 °C for 2 h; (3) cooling down at room temperature with a rate of 3 °C min^{-1}. After the reaction, the product was a white/yellow powder; the SEM-EDS grain analysis shows the presence of only Zn and S, without traces of oxidization or Fe from the reactor. Furthermore, Zn and S are detected in 1:1 atomic ratio, as expected from ZnS chemical formula. The crystal size was hundreds of nanometres and a high-resolution XRD analysis evidenced the successful synthesis of ZnS with high crystallinity.

To make further characterizations of the ZnS powder, we performed a control deposition on a silicon substrate, and we analysed it by RBS spectrometry with an alpha beam (2 MeV) at the AN2000 electrostatic accelerator in Legnaro. The RBS analysis confirmed the 1:1 stoichiometric ratio in the ZnS and the almost complete absence of ^{33,34}S contaminant isotopes in the compound. During the control deposition, the ZnS powder was also evaporated on carbon backings (nominal thickness 15 μg cm^{-2}) to form the targets used in the experiment. The RBS analysis of the control deposition gave us a thickness of the ZnS layer of 53 μg cm^{-2}, and due to the geometry of the evaporation procedure, this value corresponds also to the thickness of the deposition on the carbon backing.

2.2. The detection system

In this experiment we used the OSCAR (hOdoscope of silicon for correlations and analysis of reaction) device. OSCAR is a very compact two-stage hodoscope, which allows the isotopic identification of very low energy particles thanks to the ΔE–E telescope technique. The first detection stage of OSCAR is made by a 20 μm thick single-sided silicon strip detector; it is followed by a wall of 16 silicon pad detectors, 300 μm thick. Pre-amplifiers were cooled under vacuum via metallic contact with the walls of the chamber. All the preamplifiers were put in close connections to the detectors to reduce noise and pick-up; the silicon pad signals were directly sent to the charge preamplifiers by a plug-in connection through electronic boards. A complete description of the detector and its performances can be found in reference [Del18]. The OSCAR hodoscope was placed in the vacuum chamber onto a rotating plate (Figure 1), covering the angles from $\simeq 20 - 40^{\circ}$ in the first angular setting and $\simeq 40 - 60^{\circ}$ in the second angular setting. Polar angles were measured with an accuracy of 0.1° by means of a precision theodolite. The good granularity of the detector allows us to obtain detailed angular distributions with a single set-up of the detector, even in close-geometry experiments. The analysis of deuteron peaks of $\approx$ 5 MeV obtained in the present experiment points out to an energy resolution of $\approx$ 50 keV FWHM; according to reference [End77] and the successive literature, this among the best resolution achieved, so far, in the analysis of deuterons emitted in the ^{32}S(^{3}He, d)^{33}Cl reaction. In addition to the OSCAR device, two independent ΔE–E silicon detectors

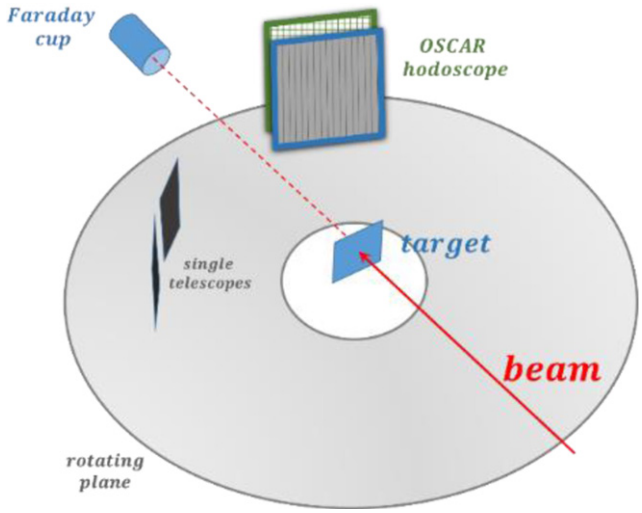

Figure 1. The OSCAR device inside the scattering chamber (on the right side of the beam line). On the left side we see the two independent ΔE–E telescopes used for check purposes.

(20–300 μm) were mounted on the opposite side of the chamber, with the purpose of making some check of the observed ejectile spectra.

2.3. Energy calibrations

A very important part of the experiment was to make accurate and reliable energy calibrations of both the detection stages. Since the silicon strip detector can show a thickness non-uniformity (see reference [Del18]), we performed two independent calibrations of the ΔE and E stages in the OSCAR telescopes. First, we calibrated the ΔE stage by means of elastic scattering of low energy ^{3}He beams on a thin ^{197}Au target.

The beam energy was varied from 2 MeV to 3.7 MeV in six steps, and six calibration points were used to calibrate the ΔE stage. We observed an excellent linearity of calibrations for all the strips. Subsequently, the beam energy was increased from 6.6 to 9.6 MeV in six steps, to allow the scattered particles to punch-through the ΔE stage. Since the energy deposited in the first stage was known thanks to the previous calibration, we performed the calibration of the second detection stage (silicon pads) *independently* of the thickness of the strip detector. Also in this case, the calibrations were almost perfectly linear. A check with pulsar signals confirmed the linearity of the electronic response. Great care was put into checking the stability of calibrations all along the experiment: the variation of the voltage drop on the bias resistor (due to the increase in the leakage current) was periodically compensated by changing the bias of the detectors and the position of several reference peaks was continuously monitored to verify possible drifts in the calibration as a function of time. The observed shifts are very low (of the order of 2‰ maximum during the whole data taking period) and have been corrected offline.

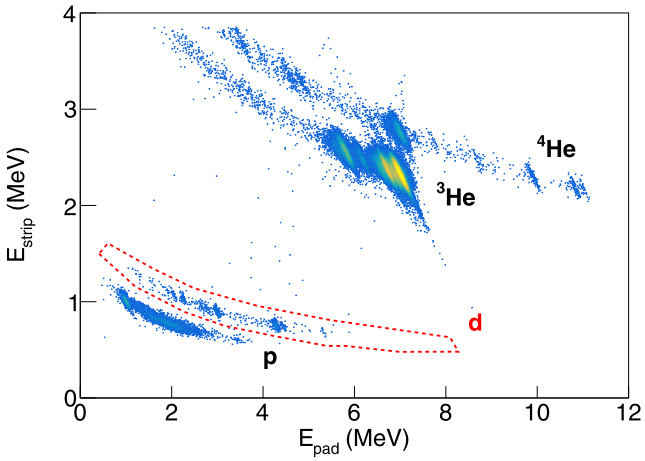

Figure 2. A ΔE–E identification matrix showing the good quality of the p, d, ^{3}He and ^{4}He identification for a pseudo-telescope of the OSCAR device. The identification threshold for deuteron is about 2 MeV.

3. Data reduction and analysis

The minimum sub-unit of the OSCAR detector is called a *pseudo-telescope*; it is made by the crossing of a given strip and a pad behind it. For each pseudo-telescope, we performed graphical cuts on the $\Delta E - E$ matrix to isolate the emission of ^{3}He and deuterons (cuts on protons and ^{4}He were also done for calibration check purposes). An example of a $\Delta E - E$ matrix obtained for a single pseudo-telescope is shown in figure 2.

To optimize the statistics, groups of pseudo-telescopes, having angles within $\pm 1^{\circ}$, were summed together to form an *angular region*. In doing that, we considered the mismatch between the orthogonal geometry of the device and the polar geometry of the reaction, as obtained from careful geometrical simulations of the experimental apparatus.

After such data reduction phases, we built a kinematical correlation plot of the emitted deuterons, where we correlated the polar angle of emission to the kinetic energy in the laboratory frame, as shown in figure 3.

A close inspection of figure 3 allows us to clearly see kinematical lines for the ^{32}S(^{3}He, d)^{33}Cl reaction, leading to the production of ^{33}Cl nucleus in the GS and in the 0.81, 2.352, 2.686 and 2.86 MeV excited states (red dashed lines). We can also see the effect due to the main reaction contaminants, ^{12}C and ^{16}O, leading to the formation of ^{13}N and ^{17}F nuclei in the ground and in the first excited state (black dashed lines). The excellent energy resolution of the detector and its good granularity, coupled with a large angular coverage, allow us also to see some faint kinematical lines (blue dashed lines) associated with reactions on ^{35}Cl nuclei present in the salt used as release agent in manufacturing the carbon backing. All these types of contaminants are commonly present in the targets used to study reactions on ^{32}S, and therefore their contributions must be carefully considered in the data analysis. To avoid any possible effect due to contaminant peaks, we considered in the data analysis only the angular region in which a given kinematical line of the ^{32}S(^{3}He, d)^{33}Cl reaction is far from a close-lying contaminant reaction by at least two standard deviations. An example of deuteron spectrum obtained at $\theta_{\mathrm{lab}} \simeq 43.7^{\circ}$ is shown in figure 4, together with the multi-gaussian fit used to extract the number of counts for each peak.

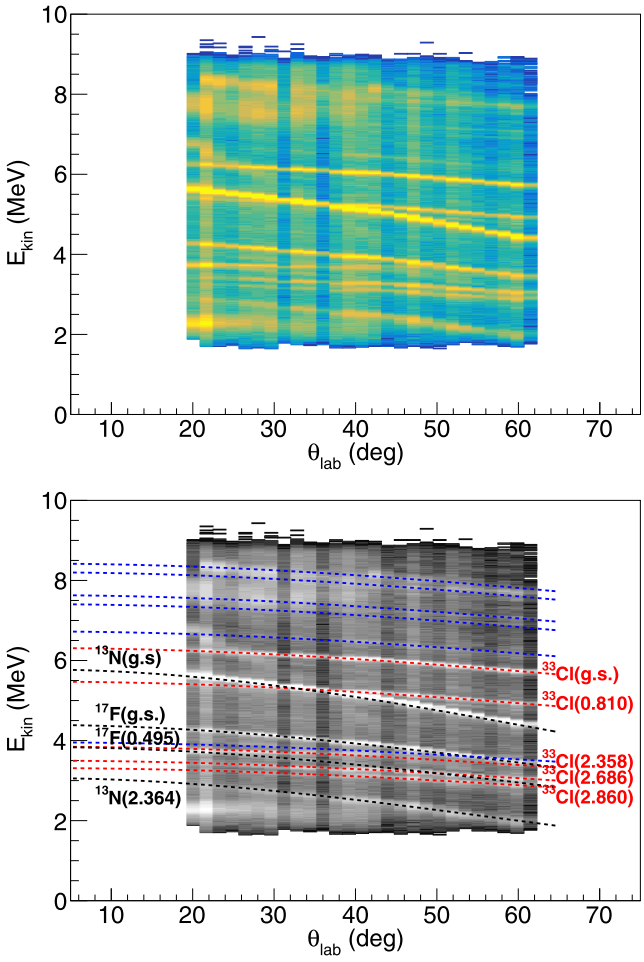

Figure 3. (Top panel) Kinematical correlation plot for deuterons detected with the OSCAR setup in the complete angular range of the experiment. The bottom panel shows a replica of the top panel in grey scale, alongside with the theoretical kinematic lines expected for: the ^{32}S(^{3}He, d)^{33}Cl reactions leading to several ^{33}Cl excited states (red dashed lines), the reactions ^{12}C(^{3}He, d)^{13}N on the backing and ^{16}O(^{3}He, d)^{17}F on oxygen contaminants (black dashed lines), and the reactions ^{35}Cl(^{3}He, d)^{36}Ar on chlorine contamination due to the release agent used for the carbon backing (blue dashed lines).

The estimate of the absolute cross section for ^{32}S(^{3}He, d)^{33}Cl reactions populating various states in ^{33}Cl was obtained by means of an *internal normalization* procedure. We verified that, at our bombarding energy, the elastic scattering of ^{3}He on Zn is fully dominated by the Coulomb component, especially at angles lower than 60° in the laboratory frame. In fact, the Coulomb barrier for such a system is about 11 MeV. Furthermore, we ran calculations of ^{3}He + ^{64,65,66}Zn with the optical model by using the Becchetti–Greenlees global parameters [Bec71], and by using the São-Paulo potential (SPP) [Cha02, Cha07, Gas07]. In both cases the deviation from the Rutherford prediction is smaller than 2% for the most backward angles, and it is vanishingly small at forward angles.

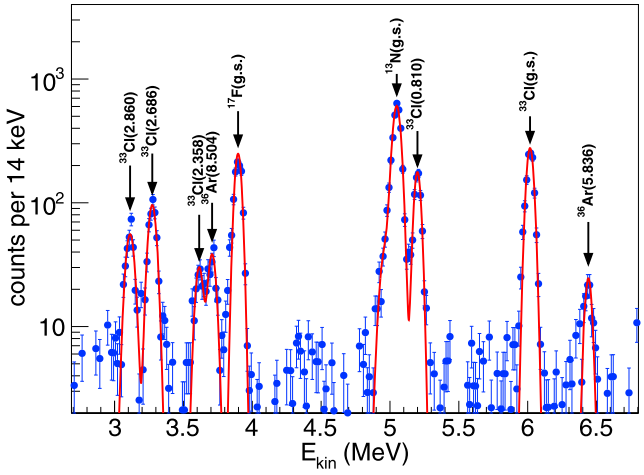

Figure 4. Multi-Gaussian fit of the deuteron spectrum obtained at $\theta_{lab} \simeq 43.7°$ with the OSCAR detector (14 keV bin). The fit concerned both the peaks associated with the ^{32}S(^{3}He, d)^{33}Cl reaction and the peaks due to the main contaminants.

Since the elastic scattering cross section on Zn is well known, and considering that we are able to extract the yield of ^{3}He particles elastically scattered by Zn nuclei (see figure 2), we derived the absolute cross section for the ^{32}S(^{3}He, d)^{33}Cl reaction by normalization to the Zn peak. We knew in fact (see section 2) that the stoichiometric ratio of the ZnS powder here used was 1:1, and therefore the numeric areal density of ^{32}S nuclei is equal to the Zn one. The internal normalization procedure allows us to estimate absolute cross sections with the lowermost errors, provided that the angles of the detectors are, as in our case, known with good accuracy. Furthermore, this normalization procedure is particularly well suited when strip detectors are used. In fact, for such type of detectors, it is generally quite difficult to determine, with good accuracy, the effective detection solid angle, that can also be affected by inter-strip effects [Gra14]. In figure 5 we show, as full dots, the angular distributions related to the feeding of the various ^{33}Cl states. The absolute cross section scales and the shapes of the observed transitions (especially for the GS and the 0.81 MeV transitions) are in reasonable agreement with the ones reported in reference [Ing75] at similar bombarding energies (10.4 MeV). In the next section, we will discuss the interpretation of the data by comparisons with finite-range DWBA and CRC calculations.

4. DWBA and CRC analysis of experimental data

We performed finite-range DWBA and CRC calculations of the ^{32}S(^{3}He, d)^{33}Cl data at 9.68 MeV bombarding energy using the FRESCO code [Tho88].

The nuclear potential is an important ingredient in the determination of the reaction mechanisms during the collision of heavy-ions [Den09]. In the present work, we have adopted the SPP interaction to describe both mass partitions involved in the ^{32}S(^{3}He, d)^{33}Cl transfer reaction: ^{3}He + ^{32}S and ^{2}H + ^{33}Cl. The SPP is a parameter-free model for the real part of the nuclear interaction. It is based on nonlocal quantum effects, which are related to the exchange of nucleons between projectile and target. The SPP presents an important predictive power of cross sections for several nuclear processes, since it is derived from a systematics for the

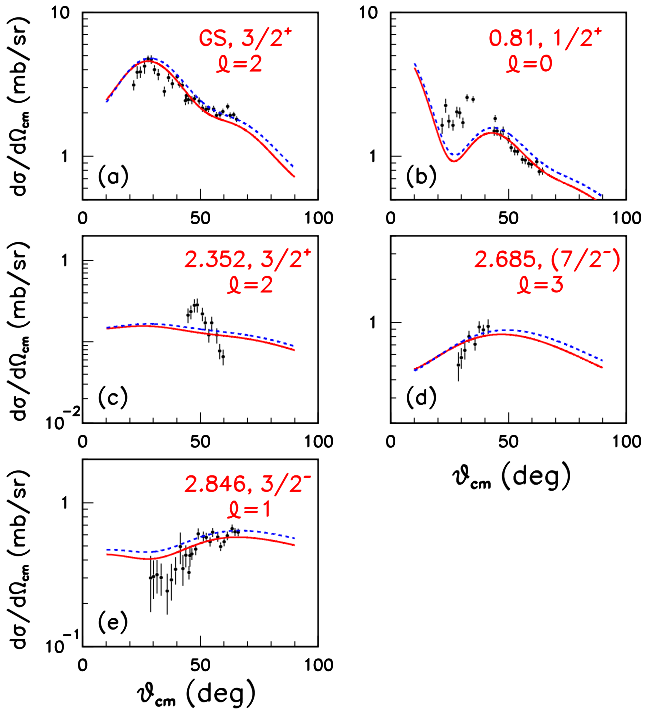

Figure 5. Angular distributions for the one-proton transfer transitions to the 0 (a), 0.81 (b), 2.352 (c), 2.685 (d) and 2.846 (e) MeV states in ^{33}Cl. Black dots: experimental data. Red solid lines: CRC calculations. Blue dashed lines: DWBA calculations.

nuclear density matter of heavy-ion nuclei [Cha02, Cha07]. In the last two decades, the SPP has been used in several studies related to nuclear physics and astrophysics [Alv03, Alv19, Ya06, Zam11].

Following the prescription adopted in reference [Per09], the imaginary potential was obtained by multiplying the strength of the SPP by a factor 0.6. To guarantee the validity of the nuclear interaction, we have performed optical model calculations for the following reactions: ^{2}H + ^{24}Mg at 12.1 MeV [Bro72], ^{2}H + ^{27}Al and ^{2}H + ^{28}Si at 12.8 MeV [Nie64], ^{3}He + ^{24}Mg at 16.0 MeV [Duh70], ^{3}He + ^{32}S at 15.0 MeV [Zur69], and ^{3}He + ^{40}Ca at 12.0 and 18 MeV bombarding energy [Abd86]. In general, the reported elastic scattering angular distributions are well described by the optical model calculations. For the reactions involving ^{3}He, we have included a spin–orbit term (Wood–Saxon shape with parameters $V_0 = 4$ MeV, $r_0 = 1.06$ fm and $a = 0.6$ fm), while for the systems with ^{2}H projectile, a tensorial potential has been included in the calculations. The shapes of the bound state wavefunctions for both the ^{3}He in the entrance channel and the ^{33}Cl in the exit channels have also been calculated by using the SPP. It is worth noting that, within this framework, the mass and charge distribution of ^{3}He are well reproduced [Ang13]. Regarding the CRC transfer calculations, no couplings to further excited states have been considered in the first partition (^{3}He + ^{32}S). For the final partition ^{2}H + ^{33}Cl, four excited states (apart from the $3/2^+$ g.s.) have been considered in the coupling scheme: $1/2^+$ at 0.810 MeV, $3/2^+$ at 2.352 MeV, $7/2^-$ at 2.685 MeV, and $3/2^-$ at 2.846 MeV. The last three states are quasi-bound states and are above the proton separation energy (2.276 MeV). In order to take into account them properly in the CRC calculations, considering them

as bound states, a procedure reported in literature was adopted (see, e.g. references [Den15, Luk14, Vin69]), i.e. to perform *approximate* DWBA and CRC calculations for *unbound* states assuming that they are bound by just 0.1 MeV. We verified that a variation of 50 keV in the bound state level did not lead to a sizeable change in the shape of the wavefunction, and therefore on the calculated cross sections. It is worth noting that the literature reports also different, more analytic, approaches to describe the quantum-mechanical properties of resonant states close to the threshold by using the so-called *Berggren representation* in the complex plane [Ber93, Lio96]; such approaches could be used in the future for some further refinements of the proton-transfer calculations here reported concerning to the $3/2^+$ state at 2.352 MeV.

Since the entrance potential was well controlled and no further states were added in the coupling scheme, the prior representation (with complex remnant) has been employed. The proton-core nuclear interactions were described by standard real Woods–Saxon potentials ($V_0 = 50$ MeV, $r_0 = 1.2$ fm and $a = 0.6$ fm). The spectroscopic factors for the target overlaps were obtained from the data fits (we reasonably assumed that the projectile/ejectile GSs overlap has a spectroscopic amplitude equal to 1).

Taking into account the predictions of the shell model for proton orbitals, in our DWBA and CRC calculations we considered one-proton transfer to the $1d_{3/2}$, $2s_{1/2}$, $2p_{3/2}$ and $1f_{7/2}$ orbitals. The results of calculations for the transitions to the various states of ^{33}Cl are reported as red (CRC) and blue-dashed lines (DWBA) in figure 5. We extracted the spectroscopic factors by a χ^2 minimization of the CRC calculations to the experimental data; the DWBA calculations shown in figure 5 are obtained by using the same spectroscopic factors. If we consider the variation of the optical model and the bound state parameters within a reasonable range of physically acceptable values, the uncertainty on the extracted spectroscopic factor amounts to about 20%. The differences between the predictions of the CRC and DWBA approaches are quite small (especially at the most forward angles), being of the order of $\approx 15\%$ maximum at backward angles.

4.1. Discussion on the spectroscopy of ^{33}Cl states

Concerning the GS transition ($3/2^+$), we suppose a transfer to the $1d_{3/2}$ orbital (with $\ell = 2$). Literature clearly indicates $\ell = 2$ as the right orbital angular momentum assignment. The CRC and DWBA calculations reproduce very well the data, except for the ones at the most forward angles. A similar effect is seen also in the data of reference [Mos70], at 12 MeV bombarding energy. A χ^2 minimization procedure leads to a spectroscopic factor $C^2S_p = 0.73$ for the GS of ^{33}Cl. This value is in excellent agreement with the one of reference [Koz72] at 29.7 MeV (0.70), while deviates up to $\approx 25\%$ with respect to the values reported in references [Ing75] (0.54) and [Mor70] (0.90). It is interesting to note that our value is not far from the values of one-neutron spectroscopic factors of the GS of the mirror nucleus ^{33}S reported in the literature (0.81 and 0.92), as indicated in references [Bob70, Mer71] and in the compilation [End77]. Our value is much closer to the prediction of the IVC model (0.77) rather than the one of the USD-shell model (0.61) [Ver94].

The population of the 0.81 MeV excited state in ^{33}Cl is attributed, with a consensus, to the proton transfer in the $2s_{1/2}$ orbital. The $\ell = 0$ nature of this transfer process will make dominant the emission of deuterons at 0°, as shown in previous works in the literature, e.g. [Ing75, Koz72]. In our work, figure 5(b), the experimental data points are mainly grouped close to the second maximum of the angular distribution, that is centred at $\theta_{cm} \simeq 40°$. Data at angles smaller than 40° show experimental cross sections larger (by a factor of $\simeq 2$) than the CRC and DWBA prediction; this trend was seen also in the [Ing75, Koz72] data, possibly indicating some inadequacy of the theoretical models in the description of the reaction mechanism. The

$C^2S_p = 0.25$ value found here is very close to the findings of references [Gra66, Ing75, Mor70] and to the predictions of the SDI (0.27) and ICV (0.28) models.

Very few data exist on the 2.352 MeV transition. In reference [Mos70], the author succeeded to measure the angular distribution (in relative units) for such a transition by using a magnetic spectrometer. He suggested a tentative $\ell = 2$ orbital angular momentum value; no C^2S_p value was reported. To our knowledge, the only existing data leading to an estimate of the C^2S_p value are the 34.5 MeV data of reference [Koz72]. In this work, the peak related to this transition was seen, in the ejectile spectrum at 30.4°, near a contaminant peak and on the tail of the huge doublet of peaks due to the 2.685 and 2.846 MeV transitions. This is a clear indication of the difficulties occurring in the detection of such a weak transition. The zero-range DWBA analysis of reference [Koz72], made by assuming a $3/2^+$ assignment for the 2.352 MeV state, led to an estimate of $C^2S_p = 0.061$, a value in good agreement with the SDI model calculation of reference [Wil71] (0.07). This value agrees also with the value (0.07) reported in reference [Elb72] by studying the ^{32}S(d, n)^{33}Cl reaction at very low energies (4.7 and 5.5 MeV)[18]. In the case of present work, for the first time, we can measure data in a region of the angular distributions that is free from effects due to close-lying contaminants. The agreement between our data and both theoretical calculations (assuming $\ell = 2$ and $J^\pi = \frac{3}{2}^+$ for the 2.352 MeV state) is not particularly good, as shown in figure 5(c). The experimental data seem to show a local bump not seen in the calculations. It is still possible (even if unlikely) that some unwanted reaction on a contaminant present in the target could pollute the small peak associated with this transition and seen in the ejectile spectrum. Another possibility could be related to the nature itself of this transition, that could be affected by a non-direct component far larger than the other ones[19]. The χ^2 minimization procedure provides a spectroscopic factor $C^2S_p = 0.073$, even if the poor agreement between data and calculations in this case leads to a larger uncertainty $\left(\approx 40\%\right)$. This value of the spectroscopic factor is similar to the previous estimate (and very close to the theoretical predictions of the SDI model [Wil71]). Since this value is involved in the indirect determination of the resonance strength of the 2.352 MeV state populated in the ^{32}S(p, γ) reaction [Ili92], it would consequently confirm the existing estimates of the reaction rate at low temperatures ($T < 0.1$ GK), which is dominated by such a narrow resonance.

The transition to the 2.685 MeV state is still the subject of some debate. In reference [Che11], two contrasting spin assignments (5/2 and 7/2) have been reported. Considering the possible angular momentum couplings, both $\ell = 2$ and $\ell = 3$ are allowed in one-proton transfer reactions. Previous works in the literature ([Ing75, Koz72, Mor70, Mos70]) tend to support the $\ell = 3$ assignment and thus the one-proton transfer to the $1f_{7/2}$ shell.

In our work, the peak associated with this transition is partially merged with a contaminant peak at the larger polar angles (see figure 3) while it is free from contaminants at the most forward angles. The $\ell = 3$ DWBA and CRC curves reasonably reproduce our experimental data; on the other hand, we observed that, if we use $\ell = 2$ and $J^\pi = \frac{5}{2}^+$ assignment in the calculations, the χ^2 value we obtain is far larger than in the $\ell = 3$ and $J^\pi = \frac{7}{2}^-$ case. This finding would support the previous suggestions reported in the literature. At the same time, it is difficult to discriminate between the possible $J^\pi = \frac{7}{2}^-$ or $\frac{5}{2}^-$ assignments that are associated to the $\ell = 3$ transfer.

[18] In the review paper [End77], this value was not included in the systematics because of the possible influence of non-direct processes at the very low bombarding energies used for the experiment.

[19] In this respect, it is interesting to observe that the transition to the close-lying (but sub-threshold) state at 1.99 MeV was reported to have a non-stripping nature in the analysis of the ^{32}S(d, n)^{33}Cl reaction at low energy reported in reference [Elb72].

Table 1. Spectroscopic properties of low-lying states in the proton-rich ^{33}Cl nucleus. The columns IV–X show the C^2S value reported in the literature (i.e. references [Gra66, Ing75, Koz72, Mor70, Ver94]) and in this work. The last column reports the unweighted average of the C^2S values and the standard deviation of the sample.

E_x in ^{33}Cl (MeV)	J^π	ℓ	[Gra66] (12 MeV)	[Mor70] (15 MeV)	[Koz72] (29.7 MeV)	[Koz72] (34.5 MeV)	[Ing75] (10.4 MeV)	[Ver94] (25 MeV)	This work (9.7 MeV)	*Average*
0	$3/2^+$	2	0.47	0.90	0.70	0.63	0.54	0.86	0.73	0.69 ± 0.16
0.81	$1/2^+$	0	0.22	0.29	0.32	0.37	0.22	0.37	0.25	0.29 ± 0.06
2.352	$3/2^+$	2	—	—	—	0.061	—	—	0.073	0.07 ± 0.01
2.685	$(7/2^-)$	3	0.52	0.73	0.50	0.41	0.52	—	0.44	0.52 ± 0.11
2.846	$3/2^-$	1	0.74	0.55	0.50	0.58	0.72	—	0.28	0.56 ± 0.17

From a qualitative point of view, it seems unrealistic that such a low energy transition would by-pass the population of the $1f_{7/2}$ (and also of the $2p_{3/2}$) shell, in favour of the $1f_{5/2}$ shell. Furthermore, the systematics show the presence of a possible analogue state in the mirror nucleus ^{33}S at 2.935 MeV, that has a $\frac{7}{2}^-$ assignment [Che11]. The $C^2S_p = 0.44$ value that we obtained (assuming the population of the $1f_{7/2}$ shell) from the CRC calculations is close to the findings of [Gra66, Ing75, Koz72].

The 2.846 MeV transition is clearly visible in the kinematical plot of figure 3. A close lying state at 2.839 MeV ($5/2^+$) has been reported in the literature, but its contribution to the transfer cross section is very small, as reported in references [Gil16, Mor70]. In the present work we reasonably assume that the kinematical line seen in figure 3 is totally due to the 2.846 MeV state. This state has a $3/2^-$ assignment, and there is a consensus in the literature that the transition has $\ell = 1$. The DWBA and CRC calculations we performed reproduce reasonably well the data (see figure 5(e)), especially at the most backward angles. We determined a $C^2S_p = 0.28$ value, which is quite smaller than the previous estimates reported in the literature at similar energies [Ing75]; we mainly attribute this difference to the smaller values of the cross section here reported.

4.2. Discussion on the C^2S values

In table 1, the C^2S value for the ^{33}Cl excited states considered in the present study are reported and compared with those obtained in previous works. The data are shown in a graphical form in figure 6, upper panel. In such a figure, we include also the values predicted from theoretical models (MSDI [Wil71], ICVM [Cas71] and USD [Ver94]).

The agreement between the various data sets is qualitative: the band of variation of the C^2S values, shown in yellow, is still quite large: up to a factor of 2 between the maximum and minimum estimates. Since the absolute C^2S values can be influenced by the different choices of optical model potentials and/or by the use of different potentials in describing the bound states, it could be useful to calculate *relative* spectroscopic factors, by normalizing the C^2S values to the GS ones. The result of such a procedure is shown, in graphical form, in figure 6 (lower panel). We can see that the discrepancies between the various data sets are reduced, especially for the lowermost energy states; anyway, a difference of a factor of ≈ 2 is persisting (and even enhanced) for the excited states at 2.685 and 2.864 MeV and would deserve some further investigations.

Following the same lines of [End77], we performed an unweighted average of the C^2S values reported in the literature, also including the results of the present work. In fact, even if C^2S

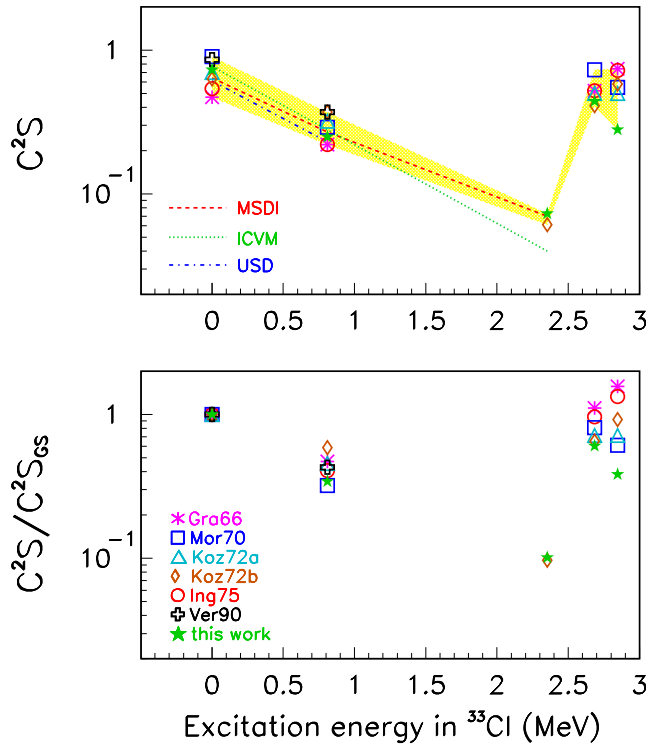

Figure 6. (Upper panel) C^2S proton spectroscopic factors for low-lying states in ^{33}Cl. Open symbols: experimental data. Asterisks: data from reference [Gra66]. Squares: data from reference [Mor70]. Triangles: data from reference [Koz72] at 29.7 MeV bombarding energy. Diamonds: data from reference [Koz72] at 34.5 MeV bombarding energy. Circles: data from reference [Ing75]. Crosses: data from reference [Ver94]. Stars: this work. (Lower panel) *relative* C^2S proton spectroscopic factors. The C^2S values for excited states in ^{33}Cl have been normalized to the GS value. The legend of symbols is as before.

values are influenced by the different choice of the adopted potential parameters, their statistical analysis can give some qualitative guidance in comparisons with theoretical calculations. The results of this procedure are shown in the last column of table 1. Concerning the bound states, the average values agree with both the SDI and ICV theoretical predictions while, just for the 2.352 MeV unbound state, the SDI prediction is in excellent agreement with the average value here reported. All the models, however, can reproduce the quoted spectroscopic factors for the *bound states* within about a standard deviation. This point indicates that further experimental efforts must be done to better discriminate between the different theoretical models.

A possibility would be to make new experiments in the 10–30 MeV bombarding energy range, preferably by using high resolution magnetic spectrometers and an isotopically pure $H_2{}^{32}S$ gas target. That is worth the risk, especially concerning a possible improvement in the estimate of the spectroscopic factor for the astrophysical important 2.352 MeV state, for which we find a C^2S_p value slightly larger than the previously reported ones.

5. Conclusions

In this paper we discussed the experimental data obtained by studying the ^{32}S(^{3}He, d)^{33}Cl one-proton transfer reaction at 9.68 MeV. A compact, high-granularity, low-threshold and high-resolution silicon hodoscope was used to detect the low energy deuteron ejectiles. A dedicated target, isotopically enriched in 32-sulphur, was manufactured; its properties were carefully tested with atomic and nuclear analyses. The large angular coverage of our hodoscope detector and the excellent energy resolution allowed us to extract the yield of one-proton transfer reactions to ^{33}Cl in its GS, 0.81, 2.352, 2.685, 2.846 MeV excited states, free from background due to contaminant reactions. Absolute cross sections were obtained with an internal normalization procedure; the obtained values are critically compared with previous measurements at similar energies. Finite-range DWBA and CRC calculations allowed us to extract the spectroscopic factors for all the transitions; their values were compared with previous findings reported in the literature, and with some nuclear structure model predictions.

The agreement between the various data sets is qualitative, with some sizeable discrepancies. Even if we average all the data of the spectroscopic factors available in the literature and obtained here, their standard deviations are still too large to allow a definitive choice between the main theoretical model (SDI, ICV, USD) predictions considered in this analysis. A slightly better agreement seems to be obtained with the SDI model predictions. Finally, it is worth noting that the spectroscopic factor obtained for the close-to-threshold state at 2.352 MeV is in reasonable agreement with the only previous estimate reported in the literature. Since the reaction rate of the ^{32}S(p, γ)^{33}Cl reaction at low temperatures $T < 0.1$ GK is fully dependent on such a value, our finding would strengthen the existing reaction rate due to this narrow state.

Acknowledgments

IL gratefully thanks Prof. A Denikin (Dubna, Russia) and Dr E Lanza (INFN, Catania) for stimulating discussions on the DWBA calculations, and acknowledge the support of the INFN-SyLiNuRe grant. We are indebted to M Loriggiola (INFN-LNL, Italy) for manufacturing high quality targets, and to L Maran and R Donolato (Univ. Padova) for delivering the ^{3}He beam at the CN accelerator in Legnaro. LRG, ALS and VABZ acknowledge supports from Fundação de Amparo à Pesquisa do Estado de São Paulo (FAPESP, Brazil) Proc. Nos. 2018/09998-8 and 2019/07767-1. DD acknowledges funding support from the Italian MIUR through the PON Ricerca e Innovazione 2014-2020, Azione I.2 A.I.M., D.D. 407/2018. We acknowledge gratefully the ENSAR2 transnational access support.

Data availability statement

The data that support the findings of this study are available upon reasonable request from the authors.

ORCID iDs

I Lombardo https://orcid.org/0000-0002-2686-9164

References

[Abd86] Abdo K M, Abdulmomen M A and Fox J D 1986 *Nucl. Phys.* A **456** 457

[Aco16] Acosta L *et al* 2016 *J. Phys.: Conf. Ser.* **730** 012001
[Alv03] Alvarez M A G *et al* 2003 *Nucl. Phys.* A **723** 93
[Alv19] Alvarez M A G *et al* 2019 *Phys. Rev.* C **100** 064602
[Ang13] Angeli I and Marinova K P 2013 *At. Data Nucl. Data Tables* **99** 69
[Aus70] Austern N 1970 *Direct Nuclear Reactions Theories* (New York: Wiley Interscience)
[Bec71] Becchetti D and Greenlees G W 1970 Polarization phenomena in nuclear reactions *Proc. Third Int. Symp.* (Madison: The University of Wisconsin Press)
[Ber93] Berggren T and Lind P 1993 *Phys. Rev.* C **47** 768
[Bij20] Bijker R and Iachello F 2020 *Prog. Part. Nucl. Phys.* **110** 103735
[Bob70] Bobrowska A *et al* 1970 *Acta Phys. Pol.* B **1** 201
[Bro72] Brown R C, Griffith J A R, Karban O, Roman S and Singh J 1972 *Nucl. Phys.* A **191** 663
[Cas71] Castel B, Stewart K W C and Harvey M 1971 *Nucl. Phys.* A **162** 273
[Cas00] Casten R F and Sherrill B M 2000 *Prog. Part. Nucl. Phys.* **45** S171
[Cha02] Chamon L C *et al* 2002 *Phys. Rev.* C **66** 014610
[Cha07] Chamon L C 2007 *Nucl. Phys.* A **787** 198
[Che11] Chen J and Singh B 2011 *Nucl. Data Sheets* **112** 1393
[Del18] Dell'Aquila D *et al* 2018 *Nucl. Instrum. Methods Phys. Res.* A **877** 277
[Del19] Dell'Aquila D *et al* 2019 *Nucl. Instrum. Methods* A **929** 162
[Den15] Denikin A S *et al* 2015 *Phys. Part. Nuclei Lett.* **12** 703
[Den09] Denikin A S, Zagrebaev V I and Descouvemont P 2009 *Phys. Rev.* C **79** 024605
[Des07] Descouvemont P 2007 *J. Phys. G: Nucl. Part. Phys.* **35** 014006
[Duh70] Duhm H H, Peterseim K, Seehars R, Finlay R and Détraz C 1970 *Nucl. Phys.* A **151** 579
[Elb72] Elbakr S A, Glavina C, Dawson W K, Gupta V K, McDonald W J and Neilson G C 1972 *Can. J. Phys.* **50** 674
[End77] Endt P M 1977 *At. Data Nucl. Data Tables* **19** 23
[Fre18] Freer M, Horiuchi H, Kanada-En'yo Y, Lee D and Meißner U G 2018 *Rev. Mod. Phys.* **90** 035004
[Gas07] Gasques L R *et al* 2007 *Phys. Rev.* C **76** 045802
[Gil16] Gillespie S 2016 Indirect studies of astrophysical reaction rates through transfer reactions *Ph D Thesis* University of York
[Gra14] Grassi L *et al* 2014 *Nucl. Instrum. Methods Phys. Res.* A **767** 99
[Gra66] Graue A 1966 *Phys. Nor.* **2** 7
[Han03] Hansen P G and Tostevin J A 2003 *Annu. Rev. Nucl. Part. Sci.* **53** 219
[HeJ18] He J-J, Lombardo I, Dell'Aquila D, Xu Y, Zhang L-Y and Liu W-P 2018 *Chin. Phys.* C **42** 015001
[Hod71] Hodgson P E 1971 *Nuclear Reactions and Nuclear Structure* (Oxford: Clarendon)
[Ili01] Iliadis C, D'Auria J M, Starrfield S, Thompson W J and Wiescher M 2001 *Astrophys. J. Suppl. Ser.* **134** 151
[Ili92] Iliadis C, Giesen U, Görres J, Wiescher M, Graff S M, Azuma R E and Barnes C A 1992 *Nucl. Phys.* A **539** 97
[Ing75] Inglima G, Caracciolo R, Cuzzocrea P, Perillo E, Sandoli M and Spadaccini G 1975 *Nuovo Cimento* A **26** 211
[Koz72] Kozub R L and Youngblood D H 1972 *Phys. Rev.* C **5** 413
[Lio96] Liotta R J, Maglione E, Sandulescu N and Vertse T 1996 *Phys. Lett.* B **367** 1
[Lom18] Lombardo I *et al* 2019 *Phys. Rev.* C **97** 034320
[Lom19] Lombardo I *et al* 2019 *Phys. Rev.* C **100** 044307
[Lom14] Lombardo I, Dell'Aquila D, Campajola L, Rosato E, Spadaccini G and Vigilante M 2014 *Bull. Russ. Acad. Sci. Phys.* **78** 1093
[Luk14] Lukyanov S M *et al* 2014 *J. Phys. G: Nucl. Part. Phys.* **41** 035102
[Mer71] Mermaz M C, Whitten C A, Champlin J W, Howard A J and Bromley D A 1971 *Phys. Rev.* C **4** 1778
[Mor70] Morrison R A 1970 *Nucl. Phys.* A **140** 97
[Mos70] Moss C E 1970 *Nucl. Phys.* A **145** 423
[Nie64] Niewodniczanski H, Nurzyinski J, Strzalkowski A, Wilczyinski J, Rook J R and Hodgson P E 1964 *Nucl. Phys.* **55** 386
[Ots20] Otsuka T, Gade A, Sorlin O, Suzuki T and Utsuno Y 2020 *Rev. Mod. Phys.* **92** 015002
[Pas17] Pastore G *et al* 2017 *Nucl. Instrum. Methods* A **860** 42

[Per09] Pereira D, Lubian J, Oliveira J R B, de Sousa D P and Chamon L C 2009 *Phys. Lett.* B **670** 330
[Pol08] Pol S V, Pol V G, Calderon-Moreno J M, Cheylan S and Gedanken A 2008 *Langmuir* **24** 10462–6
[Tho88] Thompson I J 1988 *Comput. Phys. Rep.* **7** 167
[Tho09] Thompson I J and Nunes F M 2009 *Nuclear Reactions for Astrophysics* (Cambridge: Cambridge University Press)
[Tsa05] Tsang M B, Lee J and Lynch W G 2005 *Phys. Rev. Lett.* **95** 222501
[Val19] Valdré S *et al* 2019 *Nucl. Instrum. Methods* A **930** 27
[Ver94] Vernotte J *et al* 1994 *Nucl. Phys.* A **571** 1
[Vin69] Vincent C M and Fortune H T 1969 *Bull. Am. Phys. Soc.* **14** 572
[Wil82] Wildenthal B H 1982 *Bull. Am. Phys. Soc.* **27** 725
[Wil71] Wildenthal B H, McGrory J B, Halbert E C and Graber H D 1971 *Phys. Rev.* C **4** 1708
[Yak06] Yakovlev D G *et al* 2006 *Phys. Rev.* C **74** 035803
[Zam11] Zamora J C *et al* 2011 *Phys. Rev.* C **84** 034611
[Zur69] Zurmhule R W and Fou C M 1969 *Nucl. Phys.* A **129** 502